Anal. Chem. **2008,** *80,* 2199−2203

Resonant Two-Photon Ionization Mass Spectrometry of Jet-Cooled Phenolic Acids and Polyphenols

Michael P. Callahan,† Zsolt Gengeliczki,‡ and Mattanjah S. de Vries*,†

Department of Chemistry and Biochemistry, University of California Santa Barbara, California 93106-9510, and Institute of Chemistry, Eötvös Loránd University, 1/A Pázmány P. stny. Budapest, Hungary 1117

A method for analyzing phenolic acids and polyphenols by means of resonant two-photon ionization (R2PI) mass spectrometry coupled with laser desorption and supersonic jet cooling is described. The R2PI spectra of gallic acid, 3-*O*-methylgallic acid, protocatechuic acid, syringic acid, vanillic acid, and *trans*-resveratrol are vibronically resolved and distinct to allow for unambiguous identification. For vanillic acid, its R2PI spectrum can be separated into contributions of two rotational isomers based on UV−UV and IR−UV double-resonance spectroscopy. Since R2PI spectra display sharp and well-resolved peaks, the laser wavelength can be tuned for selective ionization of targeted molecules. The mass spectrum recorded under jet-cooled conditions and at the resonant wavelength displays only the molecular ion peak with no fragmentation or background peaks. Picogram sensitivity and linear response over a nanogram range allows trace quantitative measurements of target molecules in complex matrixes. These techniques were applied to detect syringic acid in a model archaeological wine vessel.

Phenolic acids are universally distributed in plants and make up an important group of antioxidants and secondary metabolites.[1] *trans*-Resveratrol, a polyphenol, is produced by a variety of plants in response to stress and displays a wide variety of biological functions.[2,3] Great interest has developed in *trans*-resveratrol in recent years due to its anticancer[4] and antiaging[5,6] effects as well as its prevention of harmful effects from a high-caloric diet.[7] Both phenolic acids and polyphenols are important components of wine due to its organoleptic properties (e.g., flavor, astringency).[8]

The most common analytical method for detecting phenolic acids is high-performance liquid chromatography with UV−vis detection.[9] Unfortunately, the UV absorption spectra of phenolic acids are very similar and peak assignments are based mainly on retention time. Resonant two-photon ionization (R2PI) of molecules cooled in a supersonic jet expansion provides sharp, well-resolved bands with rovibronic details. The R2PI spectrum is highly dependent upon molecular structure and can distinguish between different molecules, isomers, and tautomers. We can thus target specific analytes by careful choice of wavelengths for excitation and ionization and detect these ions in a mass spectrometer. In favorable cases, this approach also greatly simplifies the mass spectrum, since only the molecule of interest will be resonantly ionized and detected.

In this paper, we present R2PI spectra of jet-cooled gallic acid, 3-*O*-methylgallic acid, protocatechuic acid, syringic acid, vanillic acid, and *trans*-resveratrol. We examine vanillic acid in further detail by UV−UV and IR−UV double-resonance spectroscopy and density functional theory (DFT) calculations. We demonstrate the use of these spectroscopic data for the analysis of wine in a model archaeological wine vessel.

EXPERIMENTAL SECTION

Gallic acid, protocatechuic acid, syringic acid, vanillic acid, and *trans*-resveratrol were obtained from Sigma-Aldrich. 3-*O*-Methylgallic acid was obtained from ChromaDex. All chemicals were used without further purification. The structures of the phenolic acids are shown in Figure 1.

The experimental setup has been described in detail elsewhere.[10] We laser desorb a thin layer of sample powder from a graphite substrate in front of a pulsed nozzle. The desorption laser, a Nd:YAG operating at 1064 nm, is attenuated to 1 mJ cm^{-2} and focused to a spot approximately 0.5 mm diameter within 2 mm in front of the nozzle orifice. We translate the graphite substrate in

* To whom correspondence should be addressed. Phone: (+1) 805-893-5921. Fax: (+1) 805-893-4120. E-mail: devries@chem.ucsb.edu.
† University of California Santa Barbara.
‡ Eötvös Loránd University.

(1) Herrmann, K. *Crit. Rev. Food Sci. Nutr.* **1989**, *28*, 315−347.
(2) Jeandet, P.; Bessis, R.; Gautheron, B. *Am. J. Enol. Vitic.* **1991**, *42*, 41−46.
(3) Langcake, P.; Pryce, R. J. *Physiol. Plant Pathol.* **1976**, *9*, 77−86.
(4) Jang, M. S.; Cai, E. N.; Udeani, G. O.; Slowing, K. V.; Thomas, C. F.; Beecher, C. W. W.; Fong, H. H. S.; Farnsworth, N. R.; Kinghorn, A. D.; Mehta, R. G.; Moon, R. C.; Pezzuto, J. M. *Science* **1997**, *275*, 218−220.
(5) Howitz, K. T.; Bitterman, K. J.; Cohen, H. Y.; Lamming, D. W.; Lavu, S.; Wood, J. G.; Zipkin, R. E.; Chung, P.; Kisielewski, A.; Zhang, L. L.; Scherer, B.; Sinclair, D. A. *Nature* **2003**, *425*, 191−196.
(6) Wood, J. G.; Rogina, B.; Lavu, S.; Howitz, K.; Helfand, S. L.; Tatar, M.; Sinclair, D. *Nature* **2004**, *430*, 686−689.
(7) Baur, J. A.; Pearson, K. J.; Price, N. L.; Jamieson, H. A.; Lerin, C.; Kalra, A.; Prabhu, V. V.; Allard, J. S.; Lopez-Lluch, G.; Lewis, K.; Pistell, P. J.; Poosala, S.; Becker, K. G.; Boss, O.; Gwinn, D.; Wang, M. Y.; Ramaswamy, S.; Fishbein, K. W.; Spencer, R. G.; Lakatta, E. G.; Le Couteur, D.; Shaw, R. J.; Navas, P.; Puigserver, P.; Ingram, D. K.; de Cabo, R.; Sinclair, D. A. *Nature* **2006**, *444*, 337−342.
(8) Arnold, R. A.; Noble, A. C.; Singleton, V. L. *J. Agric. Food Chem.* **1980**, *28*, 675−678.
(9) Robbins, R. J. *J. Agric. Food Chem.* **2003**, *51*, 2866−2887.
(10) Meijer, G.; Devries, M. S.; Hunziker, H. E.; Wendt, H. R. *Appl. Phys. B: Photophys. Laser Chem.* **1990**, *51*, 395−403.

10.1021/ac7022469 CCC: $40.75
Published on Web 02/12/2008

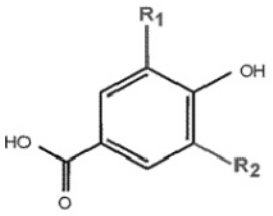

phenolic acid	R_1	R_2
gallic	OH	OH
protocatechuic	H	OH
vanillic	H	O-CH_3
syringic	O-CH_3	O-CH_3
3-O-methylgallic	OH	O-CH_3

Figure 1. Structures of the phenolic acids studied in this report.

order to expose fresh sample to successive laser shots. The nozzle consists of a pulsed valve with a nozzle diameter of 1 mm and a backing pressure of 6 atm of argon gas. The neutral molecules are skimmed and then ionized using either a one-color or two-color resonant two-photon process. The first photon from a tunable dye laser excites the molecule to an electronic excited state. Subsequently a second photon from the same (1C-R2PI) or another (2C-R2PI) tunable dye laser ionizes the molecule of interest. We detect the ions in a reflectron time-of-flight mass spectrometer. Typical mass resolution ($m/\Delta m$) is 700 or higher.

We obtain R2PI spectra by monitoring mass selected peaks while tuning the one-color, two-photon ionization wavelength. Ionization laser intensities are approximately 1 mJ pulse^{-1} and are strongly attenuated to avoid saturation. We measure UV−UV double-resonance spectra with two laser pulses separated in time by 200 ns. The first "burn" pulse removes ground state population and causes depletion in the ion signal of the second "probe" pulse, provided both lasers are tuned to a resonance of the same conformer. IR−UV double-resonance spectra are obtained in an analogous way with the burn laser operating in the near-IR region. IR frequencies are produced in an OPO system (LaserVision) pumped by a Nd:YAG laser operating at its fundamental frequency. For this work, we operated within the range of 3550−3620 cm^{-1}, which probes OH modes. Typical IR intensities in the burn region are 12 mJ pulse^{-1}, and the bandwidth is 3 cm^{-1}.

When the spectroscopy of a compound is known, we can tune the wavelength to a given resonance in order to selectively ionize it and record a mass spectrum. We observed that the graphite substrate alone does not contribute any significant signal in the mass spectrum. For analyzing sample extracts, we have developed a procedure in which we deposit samples on single-use graphite substrate discs of 2.5 mm diameter. We mount these discs on a bar that translates in vacuum, alternatingly exposing blank substrates and substrates with actual sample to the desorption laser. The desorption spot size was on the order of the graphite disc.

RESULTS AND DISCUSSION

R2PI Spectra of Phenolic Acids. Figure 2 shows one-color R2PI spectra of gallic acid, protocatechuic acid, vanillic acid, syringic acid, and 3-*O*-methylgallic acid. The R2PI spectra were recorded over a range of 287−295 nm, which was provided by frequency doubling the output of a dye laser using a mixture of R590 and R610 dyes.

Although the five phenolic acids absorb in the same wavelength region, they each have unique resonant wavelengths under the jet-cooling conditions of our experiment. These specific

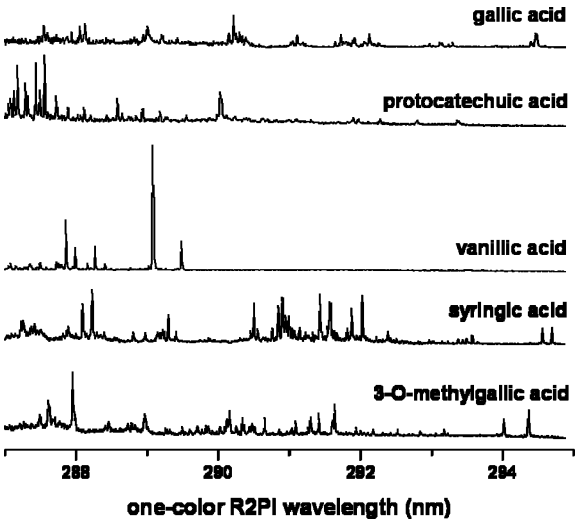

Figure 2. One-color R2PI spectra of phenolic acids.

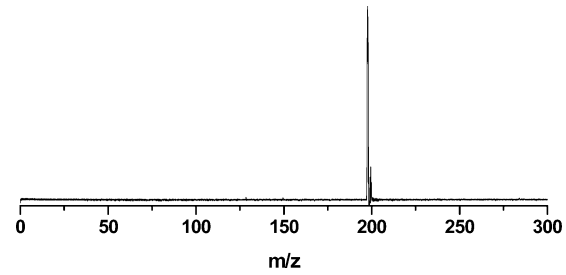

Figure 3. R2PI mass spectrum of syringic acid. Only the molecular ion and its isotope peak (M + 1) are observed allowing unambiguous identification.

resonances allow us to selectively ionize each of these components without ionizing any other compounds that may be present. Furthermore, comparison of on- and off-resonance mass spectra firmly establishes molecular identification by optical spectroscopy in addition to mass spectrometry.

This type of analysis is only possible with prior knowledge of the R2PI spectrum for the jet-cooled target molecule. The jet-cooled R2PI spectrum serves as a kind of "molecular fingerprint" since its spectral peaks are highly dependent on structure. This is clearly illustrated by examining the R2PI spectra of syringic acid and 3-*O*-methylgallic acid. These structures only differ by substituting a methoxy group with a hydroxyl group. Their R2PI spectra are very similar; however, there are distinct wavelengths between 294 and 295 nm that are sufficiently separated to allow for unambiguous identification between these two phenolic acids. Even more impressive are the structural details revealed with vanillic acid, which we discuss below.

Figure 3 shows the R2PI mass spectrum of syringic acid measured at a resonant wavelength of 288.23 nm. Only the molecular ion peak is observed in the mass spectrum. The mass spectrum is completely fragment-free; however, if fragmentation is desired for structural elucidation, increasing the laser intensity can sometimes lead to useful fragmentation. In addition, no extraneous peaks are observed from the laser desorption of the graphite matrix.

R2PI Spectrum of *trans*-Resveratrol. Orea et al. have reported the R2PI spectrum of *trans*-resveratrol measured without

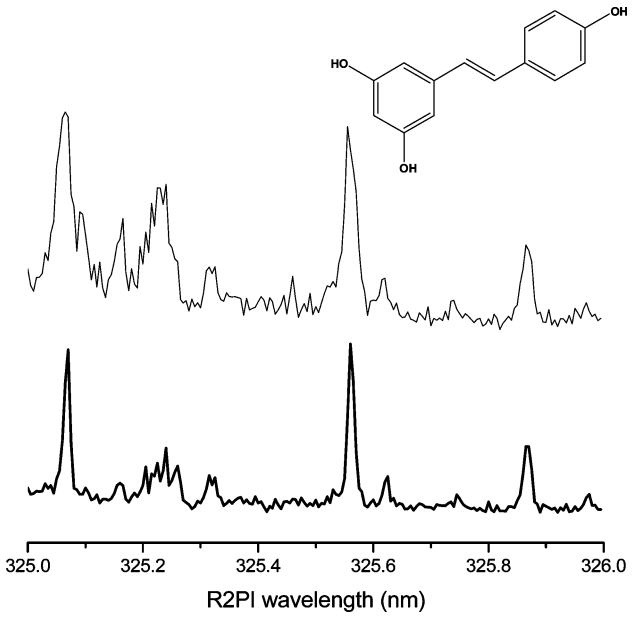

Figure 4. R2PI spectrum of *trans*-resveratrol. The top trace is measured with one-color R2PI and the bottom trace is measured with two-color R2PI with the second color set at 329 nm. The structure of *trans*-resveratrol is shown as well.

using a supersonic jet expansion.[11] Their spectrum exhibits a peak spanning from 301.5 to 307.5 nm with a maximum at 302.1 nm. This spectrum is significantly narrower when compared to the UV absorption spectrum of *trans*-resveratrol in methanol, which shows a strong, broad peak from 280 to 360 nm.

We measured the R2PI spectrum of jet-cooled *trans*-resveratrol by both one-color and two-color ionization. The spectra and the structure of *trans*-resveratrol are shown in Figure 4. The tunable UV wavelength was provided by frequency doubling the output of a dye laser using either DCM or LDS 698 laser dye. Even under jet-cooled conditions, an intense ion signal for *trans*-resveratrol was observed over a large range of UV wavelengths from 300 to 325 nm (not shown). Only in the short-wavelength range from 325 to 326 nm did we observe a sharp, well-resolved spectrum that did not contain any underlying broad absorption background.

In the one-color spectrum, some of the resonant peaks appeared slightly broadened due to power saturation. With one-color ionization, it is difficult to maximize ion production without saturating the first excitation step since the absorption and ionization cross sections usually differ by 2 orders of magnitude.[12,13] By using two-color ionization, two separate lasers allow for greater control. Thus spectral broadening due to power saturation can be reduced by proper adjustment of excitation and ionization laser intensities. In addition, selectivity can be further increased since the second photon can be tuned to just above the molecule's ionization potential. For the second color, we used 329 nm, which does not produce an ion signal by itself. The two-color R2PI of *trans*-resveratrol shows much sharper peaks at higher energies and a better signal-to-noise ratio (S/N) compared to one-color ionization. The peak widths are less than 0.02 nm (at full width at half-maximum, fwhm) under jet-cooled conditions.

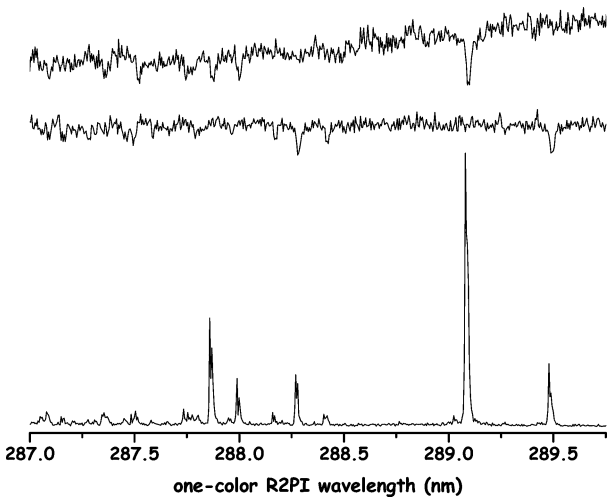

Figure 5. R2PI spectrum of vanillic acid (bottom trace) with UV−UV double-resonance spectra (top two traces). The UV−UV double-resonance spectroscopy shows two different conformational structures in this spectral region. The top trace is probed at 289.10 nm. The middle trace is probed at 289.50 nm.

UV−UV and IR−UV Double-Resonance Spectroscopy of Vanillic Acid. We further demonstrate the level of detail obtainable from the spectroscopy for the example of vanillic acid. For a complete analysis we performed UV−UV and IR−UV double-resonance spectroscopy. Figure 5 shows the R2PI spectrum of vanillic acid (bottom trace) with its UV−UV double-resonance spectra. The UV−UV double-resonance spectra were recorded with the probe laser at 289.10 nm (top trace) and 289.50 nm (middle trace). The two UV−UV double-resonance spectra are different, yet they share a similar vibronic progression suggesting two similar conformational structures. To distinguish these structures, we performed IR−UV double-resonance spectroscopy on the two vanillic acid conformers. We measured two nearly identical IR−UV double-resonance spectra at the two different wavelengths as shown in Figure 6. Both IR spectra show two strong IR bands at 3582 and 3589 cm^{-1}.

To aid in the interpretation of IR spectra, we performed DFT calculations on the four different conformers of vanillic acid. These conformers are shown in Figure 6. The conformational equilibria of vanillic acid were assessed using DFT. All calculations were carried out using the Gaussian 03 quantum code package.[14] Application of DFT's B3LYP[15−17] hybrid functional (a parametrized combination of Becke's exchange functional, the Lee, Yang, and

(11) Orea, J. M.; Montero, C.; Jimenez, J. B.; Urena, A. G. *Anal. Chem.* **2001**, *73*, 5921−5929.
(12) Boesl, U.; Neusser, H. J.; Schlag, E. W. *Chem. Phys.* **1981**, *55*, 193−204.
(13) Hager, J. W.; Wallace, S. C. *Anal. Chem.* **1988**, *60*, 5−10.
(14) Frisch, M. J.; Trucks, G. W.; Schlegel, H. B.; Scuseria, G. E.; Robb, M. A.; Cheeseman, J. R.; Montgomery, J. A., Jr.; Vreven, T.; Kudin, K. N.; Burant, J. C.; Millam, J. M.; Iyengar, S. S.; Tomasi, J.; Barone, V.; Mennucci, B.; Cossi, M.; Scalmani, G.; Rega, N.; Petersson, G. A.; Nakatsuji, H.; Hada, M.; Ehara, M.; Toyota, K.; Fukuda, R.; Hasegawa, J.; Ishida, M.; Nakajima, T.; Honda, Y.; Kitao, O.; Nakai, H.; Klene, M.; Li, X.; Knox, J. E.; Hratchian, H. P.; Cross, J. B.; Bakken, V.; Adamo, C.; Jaramillo, J.; Gomperts, R.; Stratmann, R. E.; Yazyev, O.; Austin, A. J.; Cammi, R.; Pomelli, C.; Ochterski, J. W.; Ayala, P. Y.; Morokuma, K.; Voth, G. A.; Salvador, P.; Dannenberg, J. J.; Zakrzewski, V. G.; Dapprich, S.; Daniels, A. D.; Strain, M. C.; Farkas, O.; Malick, D. K.; Rabuck, A. D.; Raghavachari, K.; Foresman, J. B.; Ortiz, J. V.; Cui, Q.; Baboul, A. G.; Clifford, S.; Cioslowski, J.; Stefanov, B. B.; Liu, G.; Liashenko, A.; Piskorz, P.; Komaromi, I.; Martin, R. L.; Fox, D. J.; Keith, T.; Al-Laham, M. A.; Peng, C. Y.; Nanayakkara, A.; Challacombe, M.; Gill, P. M. W.; Johnson, B.; Chen, W.; Wong, M. W.; Gonzalez, C.; Pople, J. A. *Gaussian 03*; Revision C.02. Gaussian, Inc.: Wallingford, CT, 2004.
(15) Becke, A. D. *J. Chem. Phys.* **1993**, *98*, 5648−5652.
(16) Lee, C.; Yang, W.; Parr, R. G. *Phys. Rev. B* **1988**, *37*, 785−789.

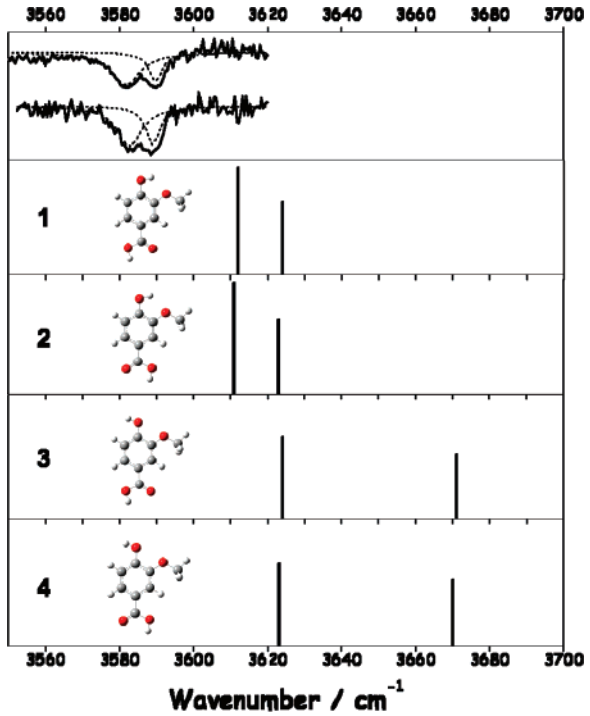

Figure 6. IR−UV double-resonance spectra of vanillic acid. The top trace is probed at 289.10 nm. The bottom trace is probed at 289.50 nm. Calculated frequencies at the B3LYP/6-31G** level are shown as stick spectra. The relative energy in kcal/mol for each conformer is 0.0 (1), 0.4 (2), 4.6 (3), and 4.9 (4). The identical IR spectra indicate two different rotational isomers (1 and 2) in the supersonic jet expansion.

Parr correlation functional and the exact exchange functional) with the 6-31G** basis set yielded equilibrium geometries of vanillic acid. We performed second-derivative calculations for purposes of vibrational frequency analysis and to verify that the geometries for all species corresponded to local minima. A corrective vibrational scaling factor of 0.9613 to B3LYP calculated frequencies was applied to account for some anharmonicity.[18]

By comparing the gas-phase IR spectrum to the calculated frequencies and intensities (also in Figure 6, as stick spectra), we conclude that rotational isomers 1 and 2 are observed in the supersonic jet expansion. The assigned rotational isomers both have intramolecular hydrogen bonds and are the lowest energy conformers as determined by DFT calculations. However, the similarity in the IR spectra impedes an exact assignment. One rotational isomer noticeably possesses higher intensity spectral peaks. Assuming both rotational isomers have similar ionization efficiencies, we assign the more intense spectrum (probed at 289.10 nm) to the lowest energy tautomer (no. 1 in Figure 6) and the less intense spectrum (probed at 289.50 nm) to the second lowest energy tautomer (no. 2 in Figure 6). However, because of its nonequilibrium nature the supersonic jet expansion may not always result in the lowest energy conformer having the highest population. Regardless, R2PI spectroscopy serves as a valuable structural probe which can discriminate between rotational isomers as well as observe intramolecular hydrogen bonding.

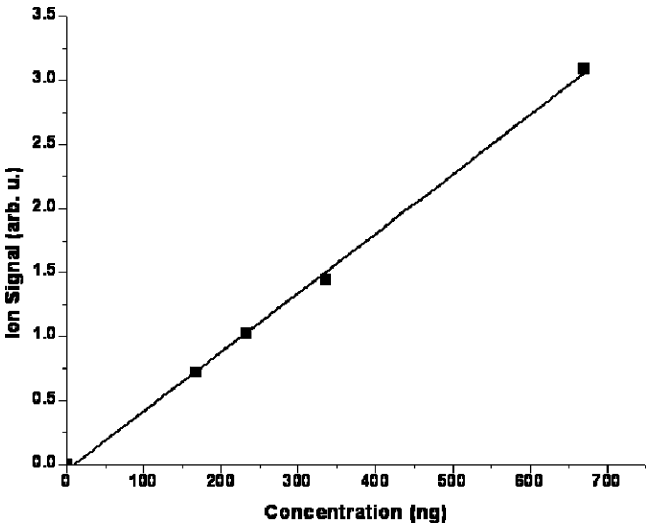

Figure 7. Linearity study measuring vanillic acid ion signal as a function of concentration.

For analytical applications, it is advantageous to identify the most stable conformational structure especially when other conformers may be present. Different conformational structures can absorb in different spectral regions, especially when intramolecular hydrogen bonding is involved (which is relevant to phenolic acids). Usually the most populated structure in the supersonic jet expansion is the lowest energy structure due to cooling. In the end, we want to tune the laser wavelength to the molecule's strongest resonant transitions. Identifying specific structures can be useful for optimizing the experimental conditions (e.g., nozzle diameter, stagnation pressure, laser delay timing) on the "best candidate". Such optimization can help in reaching the ultimate possible sensitivity for trace analysis applications

R2PI Mass Spectrometry: Linearity and Estimated Limit of Detection. We performed a linearity study using four solutions of vanillic acid in methanol, ranging in concentration from 33.5 to 134 μg/mL. We applied 5 μL of each vanillic acid solution by microsyringe onto individual graphite discs. This translated into an amount between 167.5 and 670 ng on the graphite disc. We then recorded mass spectra using an average of 10 laser shots at the most intense resonant wavelength (289.10 nm) of vanillic acid. Figure 7 shows these linearity data. The ion signal is linear with concentration (r = 0.9994), allowing (1) quantitative measurements and (2) establishment of a lower limit of detection. The latter will differ from compound to compound because it depends on the ionization efficiency. In the case of vanillic acid, we calculated our limit of detection using a mass spectrum averaged over 50 laser shots instead of 10 laser shots (not shown). With one-color ionization at 289.10 nm, we obtained a sensitivity at S/N = 3 of 60 pg per laser shot.

R2PI Mass Spectrometry: Application to Model Archaeological Residues. Specific fruits contain a variety of polyphenolic compounds.[19] Singelton has shown that anthocyanins are stable as polymers and that the associated phenolic acids can be recovered by alkaline fusion for analysis.[20,21] Singleton also

(17) Miehlich, B.; Savin, A.; Stoll, H.; Preuss, H. *Chem. Phys. Lett.* **1989**, *157*, 200−206.
(18) Foresman, J. B.; Frisch, Æ. *Exploring Chemistry with Electronic Structure Methods*; Gaussian, Inc.: Pittsburgh, PA, 1996.
(19) Ferreira, D.; Slade, D. *Nat. Prod. Rep.* **2002**, *19*, 517−541.
(20) Singelton, V. I. In *The Origins and Ancient History of Wine*; McGovern, P. E., Flemming, S. J., Katz, S. H., Eds.; Gordon and Breach: Luxembourg, 1996; pp 67−78.

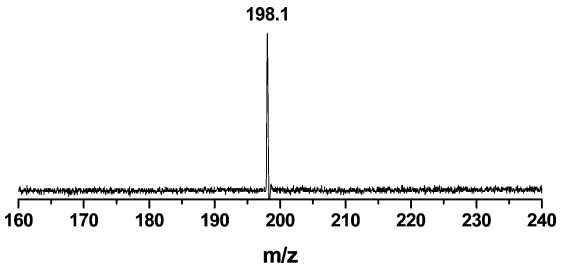

Figure 8. R2PI mass spectrum recorded at 288.23 nm of a model wine vessel treated by alkaline fusion. The mass peak at *m*/*z* 198 is assigned as syringic acid.

proposed that the ratios of phenolic acids could be informative and help differentiate wine types. For example, malvidin releases syringic acid as a unique marker of red wine.[22] Guasch-Jane and co-workers have used syringic acid detection by LC/MS/MS following alkaline fusion as a marker for red wine in amphorae from Tutankhamen's tomb.[23−25] Formenti and Duthel detected significant amounts of protocatechuic acid following alkaline fusion in wine amphorae from the shipwreck of *la Madrague in Giens* (75−60 B.C.).[26] Garnier et al. identified phenolic markers in ancient Roman amphorae by thermally assisted hydrolysis and methylation gas chromatography/mass spectrometry.[27]

We plan to use our R2PI mass spectrometry technique to study archaeological amphorae of Egyptian and Nubian origin. As proof-of-principle, we carried out model tests. Figure 8 shows the result of a model experiment in which we stored modern wine in a clay vessel until it evaporated. We subsequently broke the vessel and extracted a fragment using water/methanol (80:20, v/v), subjected the extract to an alkaline fusion procedure using KOH, and analyzed the results in our laser mass spectrometer. We recorded the mass spectrum of Figure 8 at the resonant wavelength of syringic acid, resulting in a clean mass spectrum at the parent mass. The lack of an isotope peak for syringic acid in this mass spectrum is strange, especially when we can easily observe it in Figure 3. One possible explanation is that the reproducibility of the isotope peak varies from shot-to-shot and the mass spectrum recorded in Figure 8 is only the average of five laser shots. Furthermore the resonant wavelengths differ slightly for different isotopes, affecting the observed ratios. Despite the lack of an isotope peak, syringic acid is clearly identified. This demonstrates the selective and sensitive nature of R2PI mass spectrometry and its possible application toward future archaeological sample residues.

CONCLUSIONS

We measured the R2PI spectra of jet-cooled gallic acid, 3-*O*-methylgallic acid, protocatechuic acid, syringic acid, vanillic acid, and *trans*-resveratrol. We investigated vanillic acid in further detail by UV−UV and IR−UV double-resonance spectroscopy and DFT calculations. Under our experimental conditions, two different conformational structures were determined by UV−UV double-resonance spectroscopy. We conclude that these two structures are rotational isomers based on identical IR−UV double-resonance spectra and comparison with calculated frequencies.

All of the R2PI spectra display sharp and well-resolved peaks and provide many unique resonant transitions for follow-up mass spectrometry. The mass spectrum recorded under jet-cooled conditions and at the resonant wavelength displays only the molecular ion peak with no fragmentation or background peaks. We performed a linearity study using vanillic acid demonstrating that quantitative measurements are possible with R2PI mass spectrometry. For vanillic acid, we estimate that our limit of detection is around 60 pg per laser shot with one-color R2PI. Finally, we have applied these techniques to detect syringic acid in a model archaeological wine vessel.

ACKNOWLEDGMENT

This material is based upon work supported by the National Science Foundation under Grant No. CHE-0615401. Zsolt Gengeliczki gratefully acknowledges the generous support of the Rosztoczy Foundation.

Received for review October 30, 2007. Accepted December 20, 2007.

AC7022469

(21) McGovern, P. E.; Michel, R. H. In *The Origins and Ancient History of Wine*; McGovern, P. E., Flemming, S. J., Katz, S. H., Eds.; Gordon and Breach Publishers: Luxembourg, 1996; pp 45−56.
(22) Guasch-Jane, M. R.; Ibern-Gomez, M.; Andres-Lacueva, C.; Jauregui, O.; Lamuela-Raventos, R. M. *Anal. Chem.* **2004**, *76*, 1672−1677.
(23) Guasch-Jane, M. R.; Andres-Lacueva, C.; Jauregui, O.; Lamuela-Raventos, R. M. *J. Archaeol. Sci.* **2006**, *33*, 1075−1080.
(24) Guasch-Jane, M. R.; Andres-Lacueva, C.; Jauregui, O.; Lamuela-Raventos, R. M. *J. Archaeol. Sci* **2006**, *33*, 98−101.
(25) Guasch-Jane, R.; Ibern-Gomez, M.; Andres-Lacueva, C.; Lamuela-Raventos, R. M. *Abstr. Pap.—Am. Chem. Soc.* **2003**, *225*, U73−U73.
(26) Formenti, F.; Duthel, J. M. In *The Origins and Ancient History of Wine*; McGovern, P. E., Flemming, S. J., Katz, S. H., Eds.; Gordon and Breach: Luxembourg, 1996; pp 79−85.
(27) Garnier, N.; Richardin, P.; Cheynier, V.; Regert, M. *Anal. Chim. Acta* **2003**, *493*, 137−157.